Time evolution of alignment and orientation in an electric field for the $n\ ^1D_2$ He I levels ($3 \leq n \leq 5$)

Y. Ouerdane, A. Denis, and J. Désesquelles
Laboratoire de Spectrométrie Ionique et Moléculaire, Université Lyon I, Campus de la Doua, 69622 Villeurbanne Cedex, France
(Received 16 December 1985)

The time evolution of alignment and orientation of excited atoms in an electric field is described using a density-matrix treatment. Orientation is produced by applying a tilted static electric field on levels aligned by beam-foil interaction. The modulation of polarization of the light is observed either inside the zone of constant field, by moving along the atomic beam, or downstream, in the field-free zone, by sweeping the field strength. Two different geometries are used for relative directions of ion beam, electric field vector, and foil normal. Tensor polarizabilities and cross sections for excitation of Zeeman sublevels are deduced from frequencies and amplitudes of quantum beat signals. Results are given for $n\ ^1D_2$ levels of ^{4}He I ($n = 3$, 4, and 5).

I. INTRODUCTION

Beam-foil spectroscopy is now extensively used as a spectroscopic tool. The technique is very efficient for the production of a great number of excited states of neutral and ionized atoms and the advantage of highly localized excitation is used for time evolution studies. Considerable interest in the physics of the fast-ion–foil collision has also developed. The fact that states excited by a normal foil in a cylindrical symmetry could be aligned was predicted in 1970 by Macek[1] and was soon afterwards confirmed by the quantum beat experiments of Andrä.[2] Such alignment manifests itself by the linear polarization of the light emitted by the atoms downstream of the foil. The symmetry can be broken by tilting the surface of the foil relative to the beam direction. Then the states can be oriented and the light circularly polarized. The experimental evidence of a tilt angle dependence of the beam-foil interaction was given by Berry *et al.*[3] Eck[4] presented the first model for the production of anisotropy of atoms excited by passage through a tilted foil. He assumed the existence of a strong electric field perpendicular to the foil surface. The resulting Stark effect partially transforms the initial alignment into orientation. Lombardi[5] pointed out the similarity of such a mechanism with the production of orientation by the second-order Stark effect in nonhydrogenic atoms by the action of an electric field neither parallel nor perpendicular to the beam axis.

Using the density-matrix formalism, we study the time evolution of alignment and orientation and the transfer from alignment into orientation in nonhydrogenic atoms for geometries combining either normal foil and tilted electric field or tilted foil and parallel electric field. The zones of beam-foil interaction and electric field interaction are well separated. Such time evolution and transfer are experimentally demonstrated by the modulation of linear and circular light observed along the fast particle beam in the zone of applied electric field. Alternatively, beats can be observed at a fixed distance from the foil downstream from the electric zone, in the field-free region, when sweeping the electric field strength. From the frequencies of these modulations the tensor polarizabilities of atomic states are deduced, and, from their amplitudes, cross sections for excitation of Zeeman sublevels are determined. Experiments are done with a fast helium beam excited to $n\ ^1D$ levels ($n = 3,4,5$). Preliminary results for tensor polarizability measurements in helium in normal foil and tilted electric field geometry were already reported by Ouerdane *et al.*[6]

II. TIME EVOLUTION OF POLARIZATION OF THE $n\ ^1D$ STATE

From symmetry considerations, Lombardi[7] showed that the combined action of two alignment perturbations (which separately are not statistically able to give a rotatory movement to atoms) can produce some orientation (i.e., statistically give a rotation of the atoms). For this, it is sufficient that the angle between the directions of these two alignments be different from 0° or 90°. A version of this symmetry scheme is the action of an electric field, through second-order Stark effect, on an aligned atom. This phenomenon was first studied by Lombardi and Giroud[8] in a discharge where the alignment was produced by electron bombardment, and the electric field by the external capacitors which sustained the discharge. Fast ion beam-gas collisions were also used to produce alignment.[9] In both cases, however, the electric field was parallel or perpendicular to the beam-induced alignment and a magnetic field was necessary to rotate the alignment so that orientation could appear.

Here we study, in some detail, the problem of time evolution in a pure electric field of an atom excited in a $n\ ^1D$ state by normal beam-foil interaction.

A. Density matrix evolution

Such an atom is aligned by a first perturbation which is an axially symmetrical collision. In the frame which has the collision direction as quantum axis the density matrix is simply

$$(\sigma(0))_{0xyz}=\begin{bmatrix} Q_2 & & & & \\ & Q_1 & & 0 & \\ & & Q_0 & & \\ & 0 & & Q_1 & \\ & & & & Q_2 \end{bmatrix}, \tag{1}$$

where Q_0, Q_1, and Q_2 are the cross sections for excitation of Zeeman sublevels of magnetic moments $|m_L|=0$, 1, and 2. It is easy to demonstrate that the cylindrical symmetry of excitation along the $0z$ direction has two consequences: the excitation matrix is diagonal and the diagonal elements related to opposite values of the magnetic moment m_L are equal: $\sigma_{m_L}=\sigma_{-m_L}$. The alignment appears as a difference of populations on different $|m_L|$ sublevels.

An electric field is then applied along the $0Z$ axis at 45° to the $0z$ axis. It produces a second-order perturbation which also has the symmetry of an alignment. Now the quantum axis is chosen along the electric field direction. Both axis systems are represented in Fig. 1. The excitation matrix transforms as follows:

$$(\sigma_{mm'}(0))_{0XYZ}=\sum_k R_{mk}\left[0,\frac{\pi}{4},0\right](\sigma_{kk}(0))_{0xyz} \times R^{+}_{km}\left[0,\frac{\pi}{4},0\right]. \tag{2}$$

The time evolution of the density matrix from the moment $t=0$ of application of the electric field is given, in general form, by the well-known master equation:

$$\frac{d\sigma}{dt}=-\Gamma\sigma-\frac{i}{\hbar}[\mathscr{H}_s,\sigma], \tag{3}$$

where Γ is the natural width of the excited level and $\mathscr{H}_s$ the Stark matrix. In the new reference frame $0XYZ$, the commutator of the preceding expression has the following elements:

$$[\mathscr{H}_s,\sigma]_{mm'}=\sum_{m''}\{\langle jm|\mathscr{H}_s|jm''\rangle\langle jm''|\sigma|jm'\rangle -\langle jm|\sigma|jm''\rangle\langle jm''|\mathscr{H}_s|jm'\rangle\}, \tag{4}$$

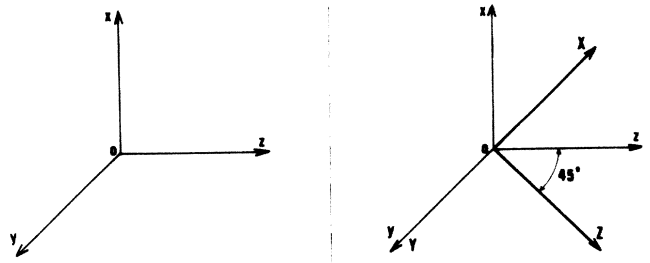

FIG. 1. Reference axes and rotation. $0z$, ion beam direction; $0y$, detection direction; $0Z$, electric field direction.

As the electric field does not couple levels of different magnetic moment,

$$\langle jm|\mathscr{H}_s|jm''\rangle=E_{m''}\delta_{mm''}. \tag{5}$$

More precisely, the Stark matrix element can be written as follows:

$$\langle jm|\mathscr{H}_s|jm'\rangle=-\frac{\alpha_{\text{tens}}}{4}\mathscr{E}^2[m^2-\tfrac{1}{3}j(j+1)]\delta_{mm'} -\frac{\alpha_{\text{sc}}}{2}\mathscr{E}^2\delta_{mm'} \tag{6}$$

where α_{sc} and α_{tens} are, respectively, the scalar and tensor polarizabilities,[10] and $\mathscr{E}$ the electric field strength; one finally obtains the solution to (3):

$$\sigma_{mm'}(t)=\sigma_{mm'}(0)e^{-\Gamma t}\exp\left[i\frac{\alpha_{\text{tens}}}{4\hbar}\mathscr{E}^2(m^2-m'^2)t\right]. \tag{7}$$

B. Density-matrix expansion on the basis of irreducible tensor operators

The transposition of results in the formalism of irreducible tensor operators simplifies the calculations and makes the interpretation easier in terms of orientation and alignment. The development of the density matrix on a basis of irreducible tensor operators is written

$$\sigma(t)=\sum_{kq}\sigma^k_q(t)T^k_q, \tag{8}$$

where the $\phi^k_q(\mathbf{e}_\lambda)$, defined by

$$(T^k_q)_{mm'}=(-1)^{j-m}\sqrt{2k+1}\begin{pmatrix} j & k & j \\ -m & q & m' \end{pmatrix}. \tag{9}$$

The orthogonality of the "$3j$" leads to the classic relation between tensor components and matrix elements of the density matrix:

$$\sigma^k_q(t)=\sum_{m,m'}(-1)^{j-m}\sqrt{2k+1}\begin{pmatrix} j & k & j \\ -m & q & m' \end{pmatrix}\sigma_{mm'}(t). \tag{10}$$

The quantities σ^k_q are more advantageous than the $\sigma_{mm'}$, since they have a more direct physical meaning[11,12] which is that σ^0_0 is proportional to the excited level population and that σ^k_q is the orientation when k is odd, and the alignment when k is even.

C. Expression for the intensity of light emitted

The light observed in the $\mathbf{k}$ direction and with the polarization $\mathbf{e}_\lambda$ has the intensity

$$I(\mathbf{k},\mathbf{e}_\lambda,t)=I_0\text{Tr}[\sigma(t)D], \tag{11}$$

where $\mathbf{e}_\lambda$ is a unit vector denoting polarization and D is the detection matrix. In the electric dipole approximation

$$D=(\mathbf{e}_\lambda\cdot\mathbf{d})(\mathbf{e}_\lambda\cdot\mathbf{d})^*, \tag{12}$$

where $\mathbf{d}$ is the electric dipole operator. D is also expanded on the T_q^k basis. The D_q^k are given as a function of the $D_{mm'}$ by an expression equivalent to (10) and the $D_{mm'}$ are given by

$$D_{mm'}=\sum_{\mu}\langle j_1 m\,|\,\mathbf{e}_\lambda\cdot\mathbf{d}\,|\,j_0\mu\rangle\langle j_0\mu\,|\,(\mathbf{e}_\lambda\cdot\mathbf{d})^*\,|\,j_1 m'\rangle\ , \quad (13)$$

where j_1 and j_0 are the angular momenta of upper and lower levels of the transition, respectively.

By projecting Eq. (11) on the tensor basis, one obtains:

$$I(k,\mathbf{e}_\lambda,t)=I_0'(-1)^{j_1+j_0}\sum_{k,q}\begin{Bmatrix}1 & 1 & k\\ j_1 & j_1 & j_0\end{Bmatrix}(-1)^q\phi_q^k\sigma_q^k(t) \quad (14)$$

where the $\phi_q^k(\mathbf{e}_\lambda)$, defined by

$$\phi_q^k(\mathbf{e}_\lambda)=\sum_{p_1,p_2}(-1)^{p_2}\sqrt{2k+1}(e_{p_1})(e_{p_2})^*\times\begin{bmatrix}1 & 1 & k\\ p_1 & -p_2 & -q\end{bmatrix}, \quad (15)$$

are simply expressed[11–13] in terms of standard components of the vector $(\mathbf{e}_\lambda)$.

D. Calculation of Stokes parameters

Finally expression (14) for the light intensity allows us to calculate the Stokes parameters I, M, C, and S,[14–16] which are sufficient to characterize the light polarization entirely.

Since we are not interested in the absolute intensity of light, we use the normalized Stokes parameters defined by

$$\frac{M}{I}=\frac{I_0-I_{90}}{I_0+I_{90}},\quad \frac{C}{I}=\frac{I_{45}-I_{-45}}{I_{45}+I_{-45}}\ ,$$

and (16)

$$\frac{S}{I}=\frac{I_{\sigma+}-I_{\sigma-}}{I_{\sigma+}+I_{\sigma+}}\ ,$$

Combining relations (2), (7), (10), (13), (14), and (16), the relative Stokes parameters are expressed as follows:

$$\frac{M}{I}=\frac{(-42Q_2+24Q_1+18Q_0)\cos(3\omega t)+6(Q_0-Q_2)\cos(\omega t)}{(57Q_2+60Q_1+43Q_0)-(9Q_2-12Q_1+3Q_0)\cos(4\omega t)}\ ,$$

$$\frac{C}{I}=-\frac{(9Q_2-12Q_1+3Q_0)-(9Q_2-12Q_1+3Q_0)\cos(4\omega t)}{(57Q_2+60Q_1+43Q_0)-(9Q_2-12Q_1+3Q_0)\cos(4\omega t)}\ , \quad (17)$$

$$\frac{S}{I}=\frac{(42Q_2-24Q_1-18Q_0)\sin(3\omega t)-18(Q_0-Q_2)\sin(\omega t)}{(57Q_2+60Q_1+43Q_0)-(9Q_2-12Q_1+3Q_0)\cos(4\omega t)}\ ,$$

where

$$\omega=-\frac{\alpha_{\text{tens}}}{4\hbar}\mathscr{E}^2\ . \quad (18)$$

We note that, in zero electric field, only M/I is nonzero.

E. Concluding remarks

In the above study we calculated the exact evolution of alignment and orientation parameters as a function of time and of the square of electric field strength. From Eq. (17) it appears that the alignment-orientation transfer is a periodic phenomenon with basic frequency ω and harmonics 3ω and 4ω.

This study was developed for the angle between initial alignment and electric field equal to 45°. The choice of another angle, provided that it differed from 0° or 90°, would change the form of these equations, but without basically modifying the transfer phenomenon.

III. EXPERIMENT

Beams of He^+ ions were produced by a 2.5-MeV Van de Graaff accelerator and collimated to a diameter of 4 mm. The beam current was held between 0.2 and 1 μA depending essentially on beam energy (200 keV–1 MeV). The carbon foil (10 ± 3 $\mu g/cm^2$), mounted on a holder having a circular aperture 8 mm in diameter, was perpendicular to the helium beam. In this first perturbation, due to cylindrically symmetric collision, only alignment of the excited atoms was possible. A second perturbation was created by an uniform electric field produced by a pair of parallel circular electrodes ($\phi=16$ cm, spacing $d=2.8$ cm) tilted at 45° to the beam. The beam was stopped in a Faraday cup. Photons emitted by excited atoms were observed at 90° to the beam direction through a circular fused silica viewing port. Light from the beam was focused by a two-lens system onto an image slit. A film polarizer, a narrow-band interference filter and, if necessary, a rotatable retarding plate, were mounted between the two lenses. The light was detected by a EMI 9635Q and EMI 9658 tubes, cooled in a Peltier-effect housing, operating in the single-photon mode. The rotation of the polarimeter was controlled by a stepping motor. Data were automatically acquired and immediately reduced by computer.

Time evolution of polarization was studied in one of two ways. In the first method the electric field was constant and variations of Stokes parameters were measured along the particle beam between the two biased plates with a good spatial resolution (Fig. 2). In this way variations of polarization are determined as a function of abscissa, i.e., directly as a function of time. In the other

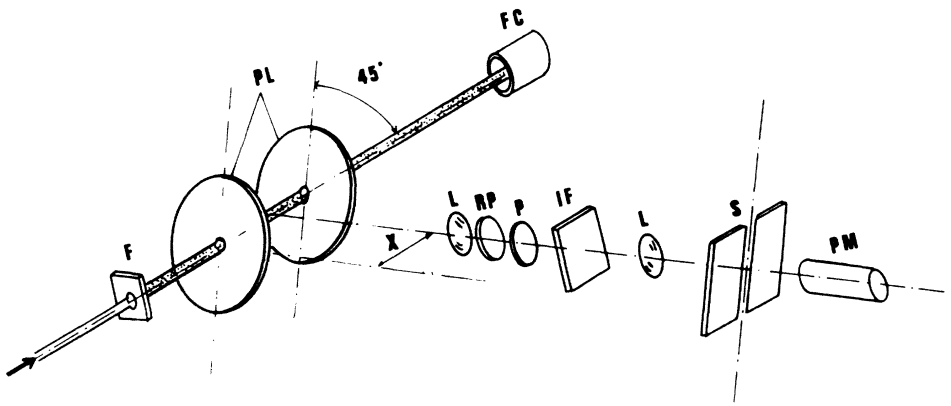

FIG. 2. Experimental arrangement: *F*, carbon foil; *FC*, Faraday cup; *PL*, electric plates; *L*, focusing lens; *RP*, retarding plate; *P*, linear polarizer; *IF*, interference filter; *S*, Slit; *X*, distance to the entrance plate.

method the observed light source was a given large volume of the beam and the Stokes parameters were measured as a function of the applied electric field strength downstream from the plates in a field-free region.

IV. NORMAL FOIL AND TILTED ELECTRIC FIELD

A. Alignment-orientation transfer

The primary aim of this work was to test the validity of the theory of orientation production from the combination of two alignments and of periodic transfer from one to the other. In order to measure the Stokes parameters we used the method proposed by Laloé[17] and developed to suit a purpose similar to ours by Berry *et al.*[15] The linear polarizer was fixed and the retarding plate was rotated by a step of 22.5°.

In Fig. 3 we show the time evolution of C/I in the $4\,^1D_2$ level of neutral helium ($4\,^1D_2$–$2\,^1P_1$ transition) directly measured in the electric field zone along the beam accelerated to 700 keV. Good spatial resolution (i.e., time resolution) is obtained by focusing beam light on a narrow slit making the photomultiplier. The interference filter has peak transmission wavelength 4922 Å. The full bandwidth at half maximum of 50 Å is sufficiently narrow to exclude other helium transitions.

The signal was small and the experiment was long and difficult. Thus we generally determined the polarization evolution by analyzing the light integrated along the beam downstream from the electric plates after removing the photomultiplier slit, keeping the observed light source abscissa fixed and sweeping the electric field strength. Statistics were much better then, as one can see in Fig. 4, where evolution of the three normalized Stokes parameters is displayed giving evidence of the progressive production of preferred alignment along the axis at 45° to the helium beam and orientation from the initial preferred alignment along the beam axis.

A good agreement between experimental results and theoretical data from expressions (17) is obtained with a suitable fit of parameters Q_0, Q_1, and Q_2.[6]

B. Tensor polarizabilities

To determine the tensor polarizability of the $n\,^1D$ ($n=3,4,5$) states of He I it is sufficient to measure one beat period of one of the three Stokes parameters. We chose the alignment M/I because of the high amplitude and the facility of measuring the linear polarization.

1. Absolute measurement ($4\,^1D$ level)

The absolute measurement requires knowledge of beam velocity, interplate distance, topography of electric field in the vicinity of plate holes, and voltage applied between plates.

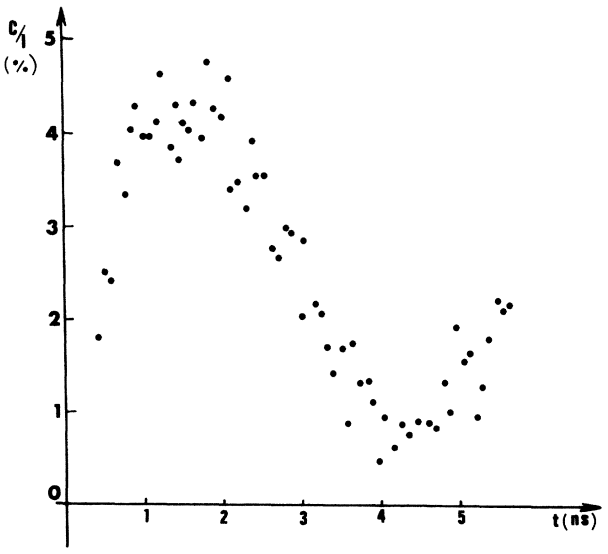

FIG. 3. Stokes parameter ratio C/I for the He I 4922 Å transition as a function of transit time in an electric field of 526 V/cm. Beam energy is 700 keV.

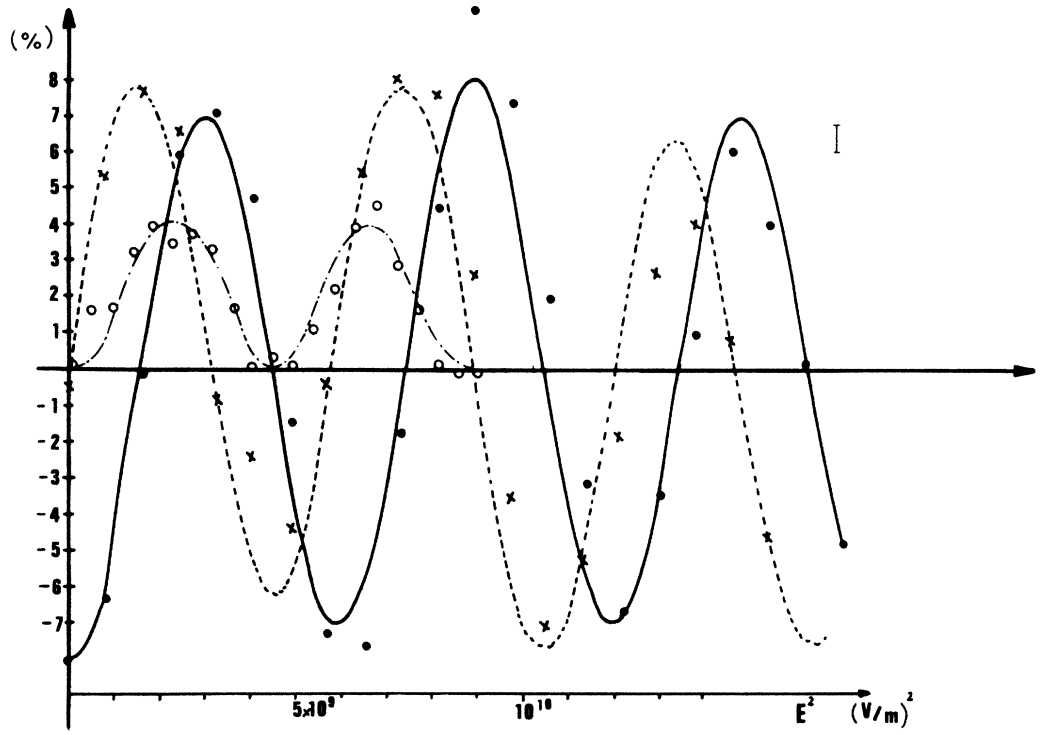

FIG. 4. Relative Stokes parameters M/I (points), C/I (circles), and S/I (crosses) of the He I 4922 Å transition as functions of the square of the electric field strength. The abscissa of the observation is downstream of the electric field region.

The beam velocity was monitored by a (p,γ) nuclear reaction and corrected for energy loss in the target.[18] The distance between plates was sufficiently precise ($\frac{1}{10}$ mm) compared to the approximation due to edge effects. These were corrected by a graphic method. The voltage applied to the plates was known with a precision of $\pm 0.2\%$.

2. *Relative measurements (3, 4, and 5 ^1D levels)*

By changing only the interference filter it is possible to make much more precise relative measurements which are free of the above-mentioned errors. Transitions $2p\,^1P$–$3d\,^1D$ (6678 Å) and $2p\,^1P$–$5d\,^1D$ (4388 Å) were selected using interference filters peaked at 6680 Å (± 140 Å) and 4381 (± 23 Å), respectively.

By measuring beats alternately from $4\,^1D$ and $(n \neq 4)\,^1D$ levels we established that results have to be corrected for thickening of the carbon foil which is proportional to beam-foil interaction time.[19] Figure 5 shows one particular experiment at 200 keV concerning the $4\,^1D$ and $5\,^1D$ levels. Light from the helium beam was observed downstream of the biased plates. The electric field was tuned so as to determine the zero value of M/I at $\frac{13}{4}$ periods for $n=5$, compared to the minimum of M/I at $\frac{1}{2}$ period for $n=4$. Our best results concerning $n=3$ and $n=4$ levels were obtained from a comparison of values of electric field corresponding to zero value of M/I at $\frac{1}{4}$ and $\frac{9}{4}$ periods, respectively. This method has the advantage of getting good statistics and precision more quickly, minimizing the frequency drift correction.

C. Excitation cross sections of Zeeman sublevels

From amplitudes of beats in electric field, the excitation cross sections Q_0, Q_1, and Q_2 can be extracted. As a matter of fact, the polarization measured in zero field is not sufficient to determine populations of Zeeman sublevels but gives only a relation between these three parameters. A second relation is given by the expression of maximum of $|C/I|$ deduced from Eq. (17):

$$\left|\frac{C}{I}\right|_{\max} = \frac{9Q_2 - 12Q_1 + 3Q_0}{33Q_2 + 24Q_1 + 23Q_0} . \tag{19}$$

We are interested in the relative value of Q_i. By introducing a normalizing equation, the following system is obtained:

$$\begin{aligned} \left|\frac{M}{I}\right|_{\mathscr{E}=0} &= \frac{-6Q_2 + 3Q_1 + 3Q_0}{6Q_2 + 9Q_1 + 5Q_0} , \\ \left|\frac{C}{I}\right|_{\max} &= \frac{9Q_2 - 12Q_1 + 3Q_0}{33Q_2 + 24Q_1 + 23Q_0} , \\ 1 &= Q_0 + 2Q_1 + 2Q_2 , \end{aligned} \tag{20}$$

Thus the energy dependence of excitation cross sections has been deduced from energy dependence of these two Stokes parameters.

The alignment data in zero field [i.e., $(M/I)_{\mathscr{E}=0}$] for

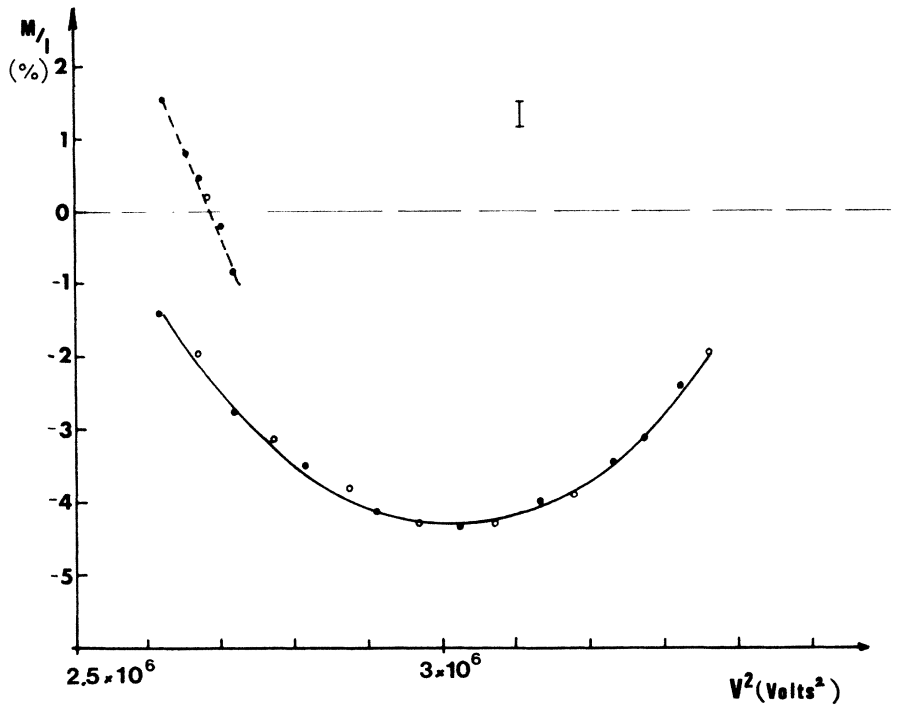

FIG. 5. Stokes parameter ratio M/I for the He I 4922 Å, ——, and 4388 Å, – – – –, transitions. Beam energy is 200 keV. ●, first run (after correction for foil thickening); ○, second run (after correction for foil thickening).

the $3\,^1D$, $4\,^1D$, and $5\,^1D$ states are shown in Figs. 6(a), 6(b), and 6(c).

To measure the maximum value of $|C/I|$ the corresponding electric field strength has to be determined. C/I is the only Stokes parameter dependent on one frequency only. A maximum is obtained for $4\omega t=\pi$. The transit time between electric plates is $t=d/(2E/m)^{1/2}$ where d is the distance between plates, E the helium beam energy, and m the mass of helium atom, and ω is proportional to the square of the electric field. The product ωt is then proportional to $\mathscr{E}^2E^{-1/2}$. Consequently the electric fields $\mathscr{E}$ and $\mathscr{E}'$ corresponding, at energies E and E', to maxima of C/I are connected by the relation

$$\mathscr{E}'=\mathscr{E}\left[\frac{E'}{E}\right]^{1/4}. \tag{21}$$

This dependence has been verified for several energies (Fig. 7) allowing us to obtain directly the dependence of the maximum of $|C/I|$ as a function of energy.

V. TILTED FOIL AND LONGITUDINAL FIELD CONFIGURATION

Edge effects are minimized and are more easily corrected if the field plates are perpendicular to the ion beam. For this purpose this geometry, where the electric field is longitudinal, has been used combined with a tilted foil. The alignment and the orientation produced at the exit surface of the carbon foil evolve in the electric field at the same frequencies as in the previous geometry. Theory is developed in a formalism similar to that given in Sec. II, with the quantum axis chosen along the beam axis direction. However the excitation matrix is more complicated and the intensity of emitted light $I(\mathbf{k},\mathbf{e}_\lambda,t)$ can be expressed easily in terms of the tensor components of the density matrix.

Using the expressions (14), (15), and (16), and taking into account the reflection symmetry in the x-z plane $[\sigma^k_{-q}=(-1)^{k-q}\sigma^k_{+q}]$, the Stokes parameters are the following:

$$\frac{M}{I}=\frac{21\sqrt{5}\sigma_0^2(0)-\sqrt{30}[3+4\cos(4\omega t)]\sigma_2^2(0)}{D},$$

$$\frac{C}{I}=\frac{2\sqrt{30}[6\cos(3\omega t)+\cos(\omega t)]\sigma_1^2(0)+i.6\sqrt{14}[2\sin(3\omega t)+\sin(\omega t)]\sigma_1^1(0)}{D},$$

$$\frac{S}{I}=\frac{6\sqrt{30}[2\sin(3\omega t)+\sin(\omega t)]\sigma_1^2(0)-i.6\sqrt{14}[2\cos(3\omega t)+3\cos(\omega t)]\sigma_1^1(0)}{D},$$

where

$$D=-20\sqrt{14}\sigma_0^0(0)+7\sqrt{5}\sigma_0^2(0)+\sqrt{30}[3+4\cos(4\omega t)]\sigma_2^2(0)$$

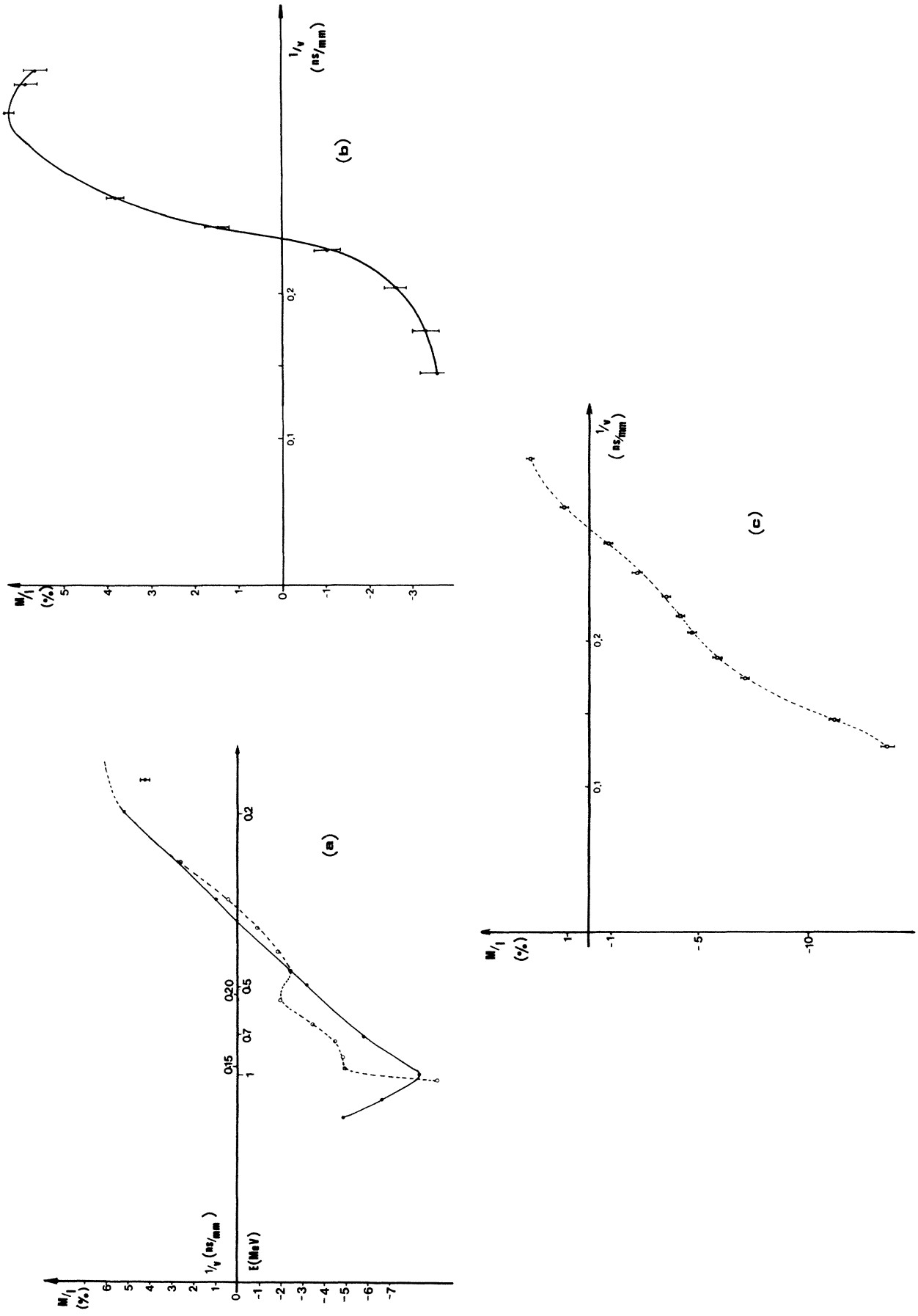

FIG. 6. Linear polarization fraction (M/I) as a function of ion energy and reciprocal beam velocity. (a) Transition $2p\ ^1P-4d\ ^1D$ at 4922 Å. Dashed line is from Schectman (Ref. 20). (b) Transition $2p\ ^1P-5d\ ^1D$ at 4388 Å. (c) Transition $2p\ ^1P-3d\ ^1D$ at 6678 Å.

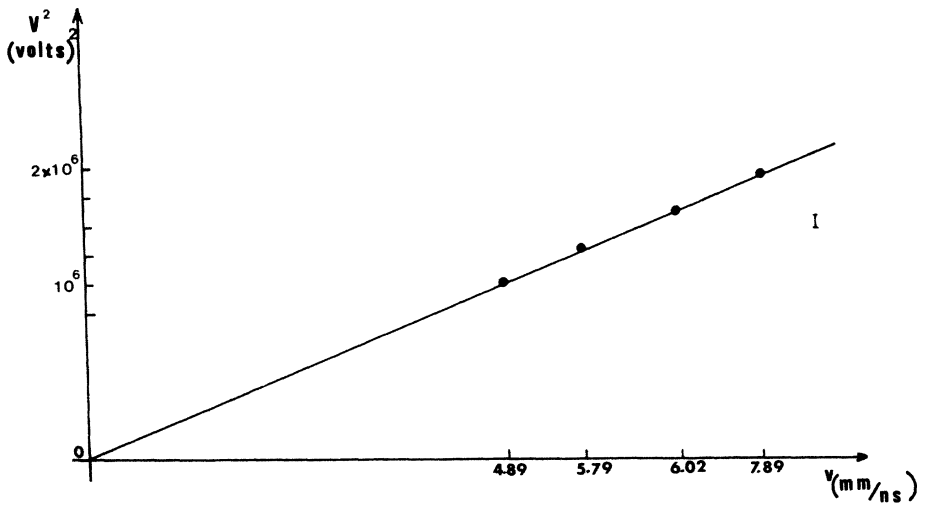

FIG. 7. Square of voltage as a function of ion velocity for the maximum value of C/I: level $4\,^1D$.

and

$$i^2=-1\ .$$

Only the linear polarization M/I is modulated at a single frequency which is 4ω. Modulation frequencies of the other Stokes parameters are ω, 3ω, and 4ω. Thus we chose to deduce the tensor polarizability from the M/I time evolution which is more conveniently analyzed.

In the particular case of a target perpendicular to the beam axis, only the $q=0$ σ_q^k components exist and

$$\left[\frac{M}{I}\right]_{\mathscr{E}=0}=\frac{21\sqrt{5}\sigma_0^2(0)}{7\sqrt{5}\sigma_0^2(0)-20\sqrt{14}\sigma_0^0(0)}$$

and

$$\frac{C}{I}=\frac{S}{I}=0\ .$$

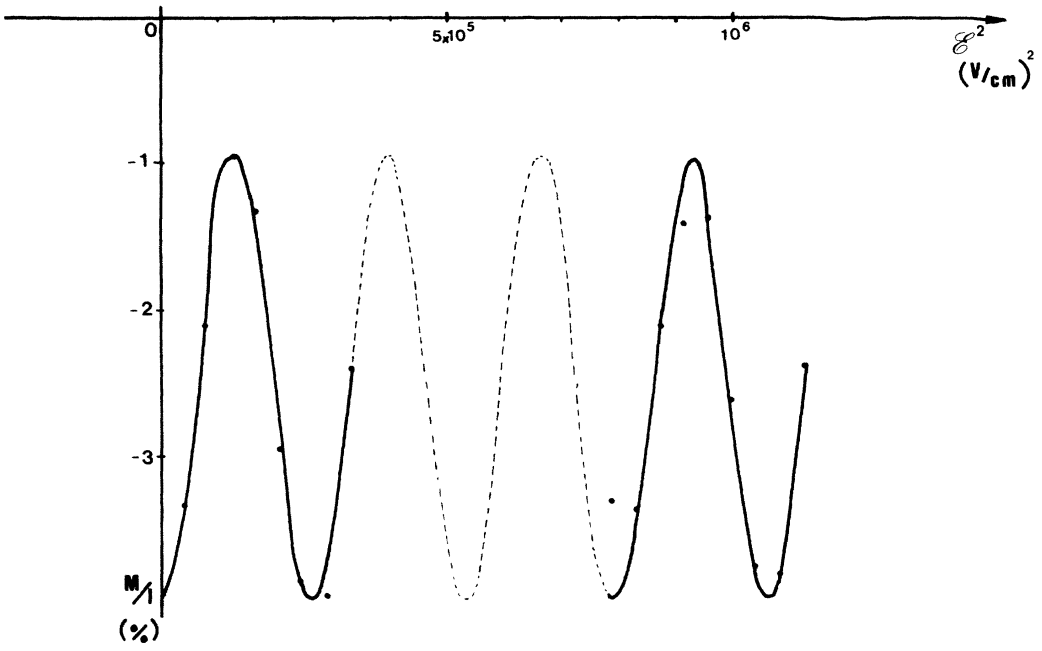

FIG. 8. Linear polarization M/I of the He I 4922 Å transition as a function of the square of the electric field strength after excitation by a tilted foil (at a tilt angle of 45°). Electric field is parallel to the helium beam axis. Energy is 250 keV. Experiment is represented by solid circles, sinusoidal fit is represented by dashed curve.

Only M/I is nonzero and its value is no longer modulated. There is no alignment-orientation transfer in an electric field applied along the beam axis when the foil is normal to the ion beam.

We have measured the linear polarization M/I of the transition $2p\ ^1P$-$4d\ ^1D$ of He I after neutralization and excitation of a He^+ beam of energy $E=250$ keV by a thin carbon foil tilted at 45° to the beam axis, and after Stark interaction with an applied electric field parallel to the beam axis. The field was produced by a pair of circular electrodes which were 16 cm in diameter and 2.95 cm in spacing. The beam was passed through holes in the electrodes and in the diaphragm placed in front of the foil; these holes were of 6 and 4 mm diameter, respectively.

For determining the Stark beat pattern of the $4\ ^1D_2$ level, the modulation of M/I was measured as a function of the applied electric field strength, downstream of the electrodes, integrating the light along a few millimeters of the helium beam. Three independent measurements have been made where alignment modulations were recorded along the first period at low field strength and along the fourth one at high field (Fig. 8).

The helium beam velocity was precisely determined from the zero-field modulation of the $2s\ ^3S-3p\ ^3P$ transition at 3889 Å. The fine structure of the $3p\ ^3P$ level is accurately known and the $^3P_2-^3P_1$ separation of 658.55 ∓ 0.15 MHz (Ref. 21) produces easily observable quantum beats at our accelerator energy. In order to increase precision in the determination of this velocity delayed quantum beats were measured far away from the target downstream of the electrodes (Fig. 9). The definition slit placed in front of the photomultiplier was also tilted at 45° to be parallel to the carbon foil. Zero-field quantum beats at 3889 Å were measured before and after the main experiment on the Stark effect in the $4\ ^1D$ level, enabling the foil thickening velocity shifts to be taken into account.

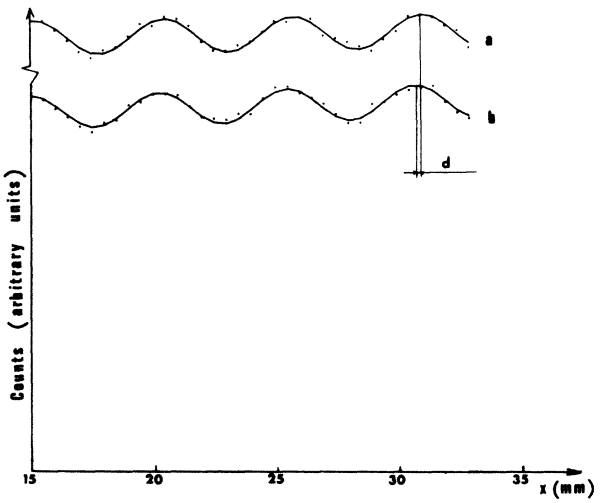

FIG. 9. Zero-field quantum beats of the He I 3889 Å transition as a function of distance from the foil. (a) First run, before the He I 4922 Å transition experiment. (b) Second run, after the He I 4922 Å transition experiment. The drift d between the two arrows is a measurement of the velocity drift of the helium due to foil thickening.

VI. RESULTS AND DISCUSSION

A. Tensor polarizabilities

Our results for tensor polarizabilities are presented together and compared with other experimental values and theoretical data in Table I. Error bars include uncertainty on electric field strength and on beam velocity and statistics.

For the $4\ ^1D$ level, beats have been measured in both geometries with about the same precision. In the tilted foil case the amplitude of modulation was much less than in the normal foil case but the beam velocity and the electric field were then more accurately determined. The level crossing data of Szostak *et al.*[22] is the only experimental value available for comparison. The level crossing technique is more complicated because it uses both electric and magnetic fields. The precision is also about 1%. Good agreement is found with calculation using the Coulomb approximation of Bates and Damgaard[23] for the electric dipole matrix elements and the compilation of Martin[24] for the level energies. In this calculation we found that the main contributions are from the nearest terms $4\ ^1P$ and $4\ ^1F$. The difference from the value ob-

TABLE I. Tensor polarizabilities [kHz/(V/cm)^2] of ^1D levels in He I. Numbers in parentheses represent the error.

	Present work			
	normal foil	tilted foil	Szostak Ref. 22	Coulomb approximation
$\alpha_{tens}(4\ ^1D)$	−0.422(5)	−0.426(4)	−0.421(6)	−0.425
$\dfrac{\alpha_{tens}(3\ ^1D)}{\alpha_{tens}(4\ ^1D)}$	0.034 40(5)		0.0311(4)	0.0331
			0.033 02[a]	
$\dfrac{\alpha_{tens}(5\ ^1D)}{\alpha_{tens}(4\ ^1D)}$	6.22(4)		6.32(10)	6.388

[a]Reference 25.

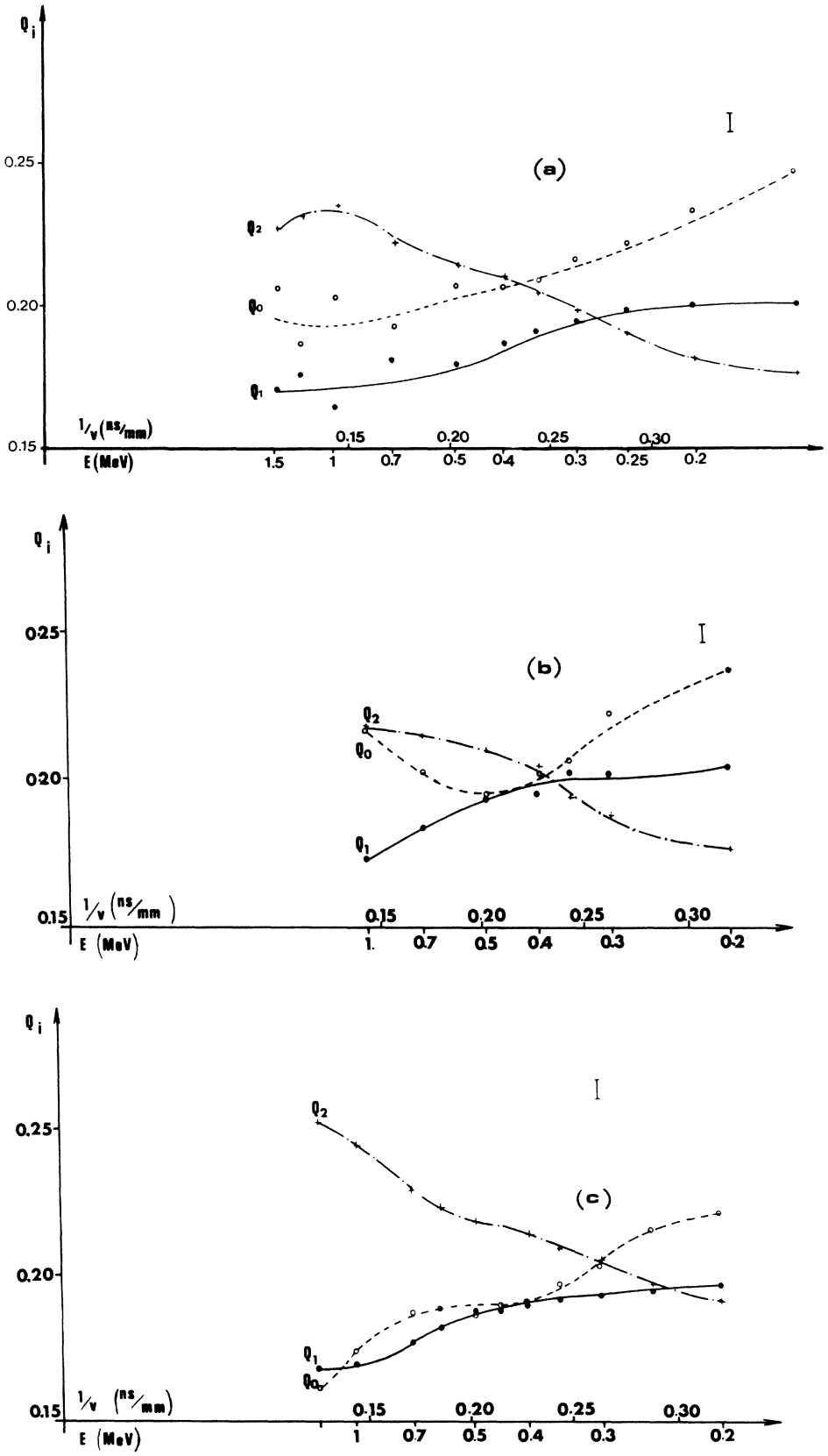

FIG. 10. Zeeman sublevel excitation cross sections Q_0, Q_1, and Q_2 as a function of reciprocal beam velocity. $Q_0+2Q_1+2Q_2=1$. (a) $4\,^1D_2$ level, (b) $5\,^1D_2$ level, (c) $3\,^1D_2$ level.

tained taking account of all $n\,^1P$ $(2 \leq n \leq 16)$ and $n\,^1F$ $(4 \leq n \leq 11)$ is only 0.1%.

Very good precision was obtained in the relative measurements due to eliminating uncertainties on the transit time and the applied electric field strength.

Tensor polarizabilities of the $3\,^1D$ and $5\,^1D$ levels have been measured by comparison with the $4\,^1D$ level only by the normal foil and tilted field technique. Our result for the $3\,^1D$ level is in poor agreement with the value published by Szostak *et al.*[22] but this latter has to be corrected following Von Oppen.[25] The result for the $5\,^1D$ level is less precise due to the weaker intensity of the $2\,^1P$–$5\,^1D$ line compared to the $2\,^1P$–$3\,^1D$ line.

B. Zeeman sublevel cross sections

Relative cross sections for the $3d\,^1D$, $4\,^1D$, and $5\,^1D$ as a function of energy are displayed in Figs. 10(a), 10(b), and 10(c).

It is found that, for the three levels, populations of sublevels $M_L = 0$ increase as energy decreases. This reproduces a result well known in the field of electron-atom collision where, at the threshold energy, only the $M_L = 0$ sublevels are populated.[1] At this low velocity the kinetic momentum, which in the entrance channel is perpendicular to the trajectory, happens to be entirely transferred to the atom because the velocity of the electron becomes zero and consequently only the component $M_L = 0$ perpendicular to the quantum axis remains. The result is not so drastic in our experiment where electrons are from the carbon foil. Moreover at these energies electronic capture is more efficient than electron excitation to produce excited states.

At high energy the polarization of transitions $2\,^1P$–$n\,^1D$ becomes negative. As in the case of electron collisions[26,27] Q_2 is larger than Q_0 and Q_1.

VII. CONCLUSION

In this work we have studied the properties of the light emitted by atoms which are aligned (and oriented) by beam-foil interaction and then are subject to the action of a static electric field which is applied at 45° to the normal to the foil surface.

We have demonstrated the transfer of alignment into orientation by second-order Stark effect. The evolution of alignment and orientation has been recorded in the electric field area along the helium beam, i.e., as a function of time and, downstream of this area, as a function of the electric field strength. From modulation frequencies, tensor polarizabilities were deduced for the $n = 3$, 4, and $5\,^1D_2$ levels of neutral helium with a precision comparable to that of level crossing results. It is shown that the Coulomb approximation of line strength is farily good even for the $n = 3$ level. From amplitudes of modulation, Zeeman sublevel excitation cross sections were determined in the energy range from 200 keV to 1.5 MeV. Results are compared to trends from simple models of collision.

The same methods are applicable to other species and other excited levels. Work on triplet levels and on hyperfine levels are under way in our laboratory.

ACKNOWLEDGMENT

The Laboratoire de Spectrométrie Ionique et Moléculaire is "Laboratoire associé No. 171 au Centre National de la Recherche Scientifique."

[1] J. Macek, Phys. Rev. A **1**, 618 (1970).
[2] H. J. Andrá, Phys. Rev. Lett. **25**, 325 (1970).
[3] H. G. Berry, L. J. Curtis, D. G. Ellis, and R. M. Schectman, Phys. Rev. Lett. **32**, 751 (1974).
[4] T. G. Eck, Phys. Rev. Lett. **33**, 1055 (1974).
[5] M. Lombardi, Phys. Rev. Lett. **35**, 1172 (1975).
[6] Y. Ouerdane, A. Denis, and J. Désesquelles, J. Phys. (Paris) Lett. **44**, L871 (1983).
[7] M. Lombardi, J. Phys. (Paris) **30**, 631 (1969); and in *Beam-Foil Spectroscopy*, edited by I. A. Sellin and D. J. Pegg (Plenum, New York, 1976), p. 731.
[8] M. Lombardi and M. Giroud, C. R. Acad. Sci., Ser. B **266**, 60 (1968).
[9] E. Chamoun, Thèse d'Etat, Université de Grenoble, 1972.
[10] J. R. P. Angel and P. G. H. Sandars, Proc. R. Soc. London, Ser. A **305**, 125 (1968).
[11] M. I. D'Yakonov, Zh. Eksp. Teor. Fiz. **47**, 2213 (1964) [Sov. Phys.—JETP **20**, 1484 (1965)].
[12] A. Omont, Prog. Quantum Electron. **5**, 69 (1977).
[13] J. P. Faroux, Thèse d'Etat, Université Paris, 1964.
[14] U. Fano and J. Macek, Rev. Mod. Phys. **45**, 553 (1973).
[15] H. G. Berry, G. Gabrielse, and A. E. Livingston, Appl. Opt. **16**, (1977).
[16] A. W. Shurcliff, *Polarized Light* (Harvard University, Cambridge, Mass., 1966).
[17] F. Laloë, Ann. Phys. (N.Y.) **6**, 5 (1971).
[18] J. F. Ziegler, *Helium Stopping Powers and Ranges in all Elements* (Pergamon, New York, 1977), Vol. 4.
[19] Y. Ouerdane, Thèse de 3ème Cycle, Université de Lyon I, 1983.
[20] R. M. Schectman, L. J. Curtis, and H. G. Berry, in *Proceedings of the Fifth Fast Ion Spectroscopy International Conference on Beam-Foil Spectroscopy, Lyon, 1978,* edited by J. Désesquelles [J. Phys. (Paris) **2**, C1-289 (1978)].
[21] J. Wieder and W. E. Lamb, Jr., Phys. Rev. **107**, 125 (1957).
[22] D. Szostak, G. Von Oppen, and W. D. Perschmann, Phys. Lett. **76A**, 376 (1980).
[23] D. R. Bates and A. Damgaard, Philos. Trans. R. Soc. London Sci., Ser. A **242**, 101 (1949).
[24] W. C. Martin, J. Phys. Chem. Solids, Suppl. **2**, 257 (1973).
[25] G. Von Oppen, W. Schilling, and Y. Kriescher, Z. Phys. A **321**, 91 (1985).
[26] E. W. Lamb, Jr., Phys. Rev. **105**, 559 (1957).
[27] I. C. Percival and M. J. Seaton, Philos. Trans. R. Soc. London, Ser. A **251**, 114 (1958).